



HAL
open science

The reaction of $M(\text{CO})_3(\text{Ph})_2\text{PCH}_2\text{CH}_2\text{PPh}_2$ ($M = \text{Fe}, \text{Ru}$) with parahydrogen: probing the electronic structure of reaction intermediates and the internal rearrangement mechanism for the dihydride products

Danièle Schott, Philip Callaghan, John Dunne, Simon Duckett, Cyril Godard, José Goicoechea, Jeremy Harvey, John. Lowe, Roger Mawby, Georg Müller, et al.

► **To cite this version:**

Danièle Schott, Philip Callaghan, John Dunne, Simon Duckett, Cyril Godard, et al.. The reaction of $M(\text{CO})_3(\text{Ph})_2\text{PCH}_2\text{CH}_2\text{PPh}_2$ ($M = \text{Fe}, \text{Ru}$) with parahydrogen: probing the electronic structure of reaction intermediates and the internal rearrangement mechanism for the dihydride products. Dalton Transactions, 2004, 20, pp.3218-3224. 10.1039/B407457B . hal-03278472

HAL Id: hal-03278472

<https://hal.science/hal-03278472>

Submitted on 7 Jul 2021

HAL is a multi-disciplinary open access archive for the deposit and dissemination of scientific research documents, whether they are published or not. The documents may come from teaching and research institutions in France or abroad, or from public or private research centers.

L'archive ouverte pluridisciplinaire **HAL**, est destinée au dépôt et à la diffusion de documents scientifiques de niveau recherche, publiés ou non, émanant des établissements d'enseignement et de recherche français ou étrangers, des laboratoires publics ou privés.

The reaction of $M(\text{CO})_3(\text{Ph}_2\text{PCH}_2\text{CH}_2\text{PPh}_2)$ ($M = \text{Fe}, \text{Ru}$) with parahydrogen: probing the electronic structure of reaction intermediates and the internal rearrangement mechanism for the dihydride products

Danièle Schott,^a Philip Callaghan,^a John Dunne,^a Simon B. Duckett,^{a*} Cyril Godard,^a José M. Goicoechea,^d Jeremy N. Harvey,^b Roger J. Mawby,^a Georg Müller,^a Robin N. Perutz,^a Rinaldo Poli^c and Michael K. Whittlesey^d

^a Department of Chemistry, University of York, YO10 5DD, United Kingdom, sbd3@york.ac.uk

^b Department of Chemistry, University of Bristol, BS8 1TS, United Kingdom

^c Laboratoire de Chimie de Coordination, 205 Route de Narbonne, 31077 Toulouse Cedex, France

^d Department of Chemistry, University of Bath, Claverton Down, Bath BA2 7AY, United Kingdom

*This submission was created using the RSC Article Template (DO NOT DELETE THIS TEXT)
(LINE INCLUDED FOR SPACING ONLY - DO NOT DELETE THIS TEXT)*

The photochemical reaction of $\text{Ru}(\text{CO})_3(\text{dppe})$ and $\text{Fe}(\text{CO})_3(\text{dppe})$ ($\text{dppe} = \text{Ph}_2\text{PCH}_2\text{CH}_2\text{PPh}_2$) with parahydrogen has been studied by *in situ*-photochemistry resulting in NMR spectra of $\text{Ru}(\text{CO})_2(\text{dppe})(\text{H})_2$ that show significant enhancement of the hydride resonances while normal signals are seen in $\text{Fe}(\text{CO})_2(\text{dppe})(\text{H})_2$. This effect is associated with a singlet electronic state for the key intermediate $\text{Ru}(\text{CO})_2(\text{dppe})$ while $\text{Fe}(\text{CO})_2(\text{dppe})$ is a triplet. DFT calculations reveal electronic ground states consistent with this picture. The fluxionality of $\text{Ru}(\text{CO})_2(\text{dppe})(\text{H})_2$ and $\text{Fe}(\text{CO})_2(\text{dppe})(\text{H})_2$ has been examined by NMR spectroscopy and rationalised by theoretical methods which show that two pathways for ligand exchange exist. In the first, the phosphorus and carbonyl centres interchange positions while the two hydride ligands are unaffected. A second pathway involving interchange of all three ligand sets was found at slightly higher energy. The H-H distances in the transition states are consistent with metal-bonded dihydrogen ligands. However, no local minimum (intermediate) was found along the rearrangement pathways.

Introduction

Reactions implicating more than one electronic state are relatively common. In view of the differing rates of singlet-singlet and singlet-triplet combinations, the existence of the two spin states can affect product distributions significantly. It is also possible that while both reagents and products have the same electronic spin state, spin crossover occurs during the transformation and a highly complex reaction pathway is followed. Although breakthroughs have been made in the spectroscopic examination of reaction intermediates, their short lifetime makes detailed study experimentally challenging. One reaction that has been studied in great detail is the oxidative addition of H_2 to $\text{Fe}(\text{CO})_4$.¹⁻⁴ Experimentally it has been shown that rate of H_2 addition to triplet $\text{Fe}(\text{CO})_4$ is three orders of magnitude slower than that to related singlet states.⁵ This phenomenon has been attributed to the spin forbidden character of the singlet-triplet combination. The chemistry of the group 6 metallocenes, $(\eta^5\text{-C}_5\text{H}_5)_2\text{W}$ and their *ansa*-bridged analogues that can be generated photochemically from the corresponding dihydrides^{6a} or methyl hydrides^{6b} is also dominated by singlet/triplet effects.⁷ A further example is provided by $(\eta^5\text{-C}_5\text{H}_5)\text{Co}(\text{CO})$, formed by photolysis of $(\eta^5\text{-C}_5\text{H}_5)\text{Co}(\text{CO})_2$.⁸ This species is a spin triplet whereas its rhodium and iridium analogues have singlet ground states. Remarkably, triplet $(\eta^5\text{-C}_5\text{H}_5)\text{Co}(\text{CO})$, proves to be the most reactive species towards Si-H activation. Theoretical analyses of $(\eta^5\text{-C}_5\text{H}_5)\text{Co}(\text{CO})$ and $(\eta^5\text{-C}_5\text{H}_5)\text{Co}(\text{CO})\text{L}$ ($\text{L} = \text{PH}_3$ and C_2H_4) support triplet ground states for these species.^{8,9} Understanding how such electronic changes influence a metal centre's potential to cleave the C-H bond of an alkane remains an important goal in C-H bond functionalisation.¹⁰

In many ways, NMR spectroscopy is an ideal technique for studying solution based reactions, since most elements exhibit at least one NMR-active isotope, and isotopic labelling can be undertaken if greater sensitivity is required. Nevertheless, NMR spectroscopy remains a technique with low sensitivity that is hard to adapt to the study of short-lived

species. One route that increases the sensitivity of the NMR experiment involves the use of parahydrogen ($p\text{-H}_2$).¹¹ This leads to the observation of substantially enhanced signals for nuclei that originate in the $p\text{-H}_2$ molecule or couple to these nuclei. The effect has been called Parahydrogen Induced Polarisation (PHIP) or PASADENA (Parahydrogen And Synthesis Allow Dramatically Enhanced Nuclear Alignment) and has been extensively reviewed.¹¹⁻¹⁵

In this paper we employ the parahydrogen effect in conjunction with *in-situ* photolysis¹⁶ to study reaction intermediates. Several groups have demonstrated how UV photolysis of an NMR sample within the NMR probe can be used to generate new materials.^{16,17} Reports also describe how this method enables species to be characterised that might normally be considered reaction intermediates by conducting experiments at temperatures low enough to extend their lifetime substantially.¹⁶ Here, we use a 325 nm He-Cd continuous wave laser to generate intermediates that yield metal dihydride complexes upon reaction with H_2 .¹⁸ When $p\text{-H}_2$ is used the electronic structure of the reaction intermediate is shown to be indicated by key features of the resultant NMR spectra of the reaction product, even though the reaction intermediate itself is not directly observed. Density functional theory (DFT) is used to confirm the electronic structure of these intermediates and map the reaction pathways.

Results and Discussion

Reaction of $p\text{-H}_2$ with $\text{Ru}(\text{CO})_2(\text{dppe})$ and $\text{Fe}(\text{CO})_2(\text{dppe})$. We have previously reported that $\text{Ru}(\text{CO})_3(\text{dppe})$ ($\text{dppe} = \text{Ph}_2\text{PCH}_2\text{CH}_2\text{PPh}_2$) reacts with $p\text{-H}_2$ under photolytic conditions at 295 K to yield enhanced signals for the corresponding dihydride $\text{Ru}(\text{CO})_2(\text{dppe})(\text{H})_2$ **1** (Figure 1a).¹⁸ This observation can be reproduced at 203 K. Since $p\text{-H}_2$ corresponds to H_2 in the anti-symmetric nuclear spin state ($\alpha\beta\text{-}\beta\alpha$), any reaction that leads to a product in which this spin encoding is retained, will yield NMR signals that are derived

from a non-Boltzmann spin population. When this process is described using the product operator formalism, the resultant $I_z S_z$ product state leads to $I_z S_x$ and $I_x S_z$ terms upon interrogation. Each of these terms corresponds to an anti-phase signal, one for the I spin and one for the S spin, which are separated by J_{IS} which in this case corresponds to J_{HH} . However, when the

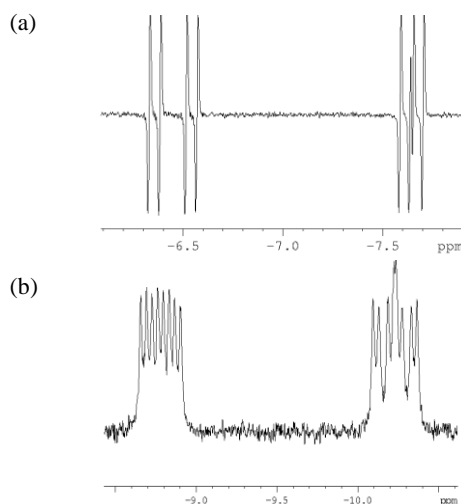
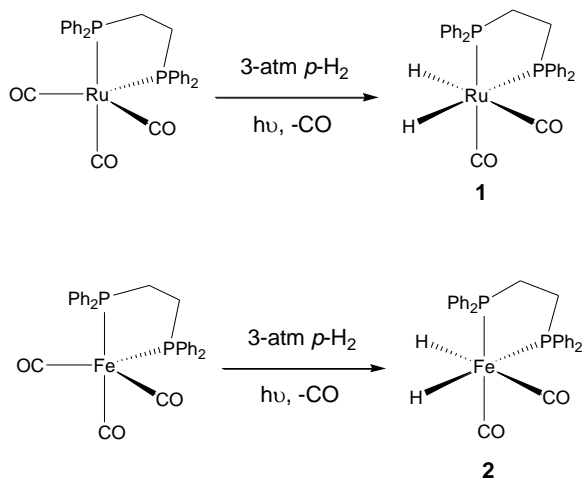


Figure 1. Hydride signals observed by *in situ* UV photolysis of $M(\text{CO})_3(\text{dppe})$ in the presence of 3 atm of $p\text{-H}_2$: (a) $M=\text{Ru}$, (b) $M=\text{Fe}$.

related ^{13}C labelled iron complex $\text{Fe}(^{13}\text{CO})_5$ was photolysed with $p\text{-H}_2$ no enhanced hydride resonances were observed for $\text{Fe}(^{13}\text{CO})_4(\text{H})_2$. This result is surprising since the ^{13}C label forces the hydride ligands to belong to a second order spin system and $p\text{-H}_2$ activity is expected. Such an enhancement has already been reported by ourselves when *cis-trans-cis* $\text{Ru}(^{13}\text{CO})_2(\text{PMe}_3)_2(\text{H})_2$ undergoes thermally driven H_2 exchange with $p\text{-H}_2$.¹⁸ It is generally accepted that the un-solvated 16-electron intermediate $\text{Fe}(\text{CO})_4$ adopts a triplet ground state while related $\text{Ru}(0)$ species are expected to have singlet ground states.² We therefore postulated that quenching of the $p\text{-H}_2$ spin state would occur during the addition of H_2 to $\text{Fe}(\text{CO})_4$ and that this accounts for the failure to detect any signal enhancement. This simple observation is, however, complicated by the known fluxionality of $\text{FeL}_4(\text{H})_2$ ($L = 2$ electron donor) systems which could also quench the antiphase signal by excessive line broadening.¹⁹

In order to carry out a definitive experiment, the analogous iron complex $\text{Fe}(\text{CO})_3(\text{dppe})$ was prepared and a sample continuously photolysed at 203 K with $p\text{-H}_2$ whilst appropriate NMR spectra were recorded. The immediate generation of the known dihydride $\text{Fe}(\text{CO})_2(\text{dppe})(\text{H})_2$ **2** was indicated by the observation of two hydride resonances as

doublets of doublets of doublets centred at $\delta -8.8$ ($|^2J_{\text{HH}}| = 14.5$ Hz, $|^2J_{\text{PH}}| = 28.5$ Hz and 56.4 Hz) and $\delta -10.24$ ($|^2J_{\text{HH}}| = 14.5$ Hz, $|^2J_{\text{PH}}| = 35.4$ Hz and 57.4 Hz).²⁰ These signals had normal phase profiles (Figure 1b), and no evidence for $p\text{-H}_2$ amplification was evident. A solution containing a mixture of $\text{Ru}(\text{CO})_3(\text{dppe})$ and $\text{Fe}(\text{CO})_3(\text{dppe})$ under 3-atmospheres of $p\text{-H}_2$ was also prepared and irradiated in CD_3CN at 243 K. The hydride signals for the ruthenium dihydride **1** were still enhanced, while those for **2** again showed normal shape. The most logical explanation for this effect requires different electronic spin states at the metal. We changed to the more coordinating solvent because we expected the Fe reaction to proceed via the solvent complex $\text{Fe}(\text{CO})_2(\text{dppe})(\text{CD}_3\text{CN})$ which was expected to be a singlet. Although *para*-hydrogen induced polarisation was observed for **1**, the signals for **2** were unaffected, and fast depletion of the *para*-hydrogen reservoir was observed. This suggests that $\text{Fe}(\text{CO})_2(\text{dppe})(\text{CD}_3\text{CN})$ rapidly accesses the naked metal fragment which is involved in reaction with H_2 .

Characterisation of $\text{Fe}(\text{CO})_2(\text{dppe})(\text{H})_2$ (2**).** In order to characterise $\text{Fe}(\text{CO})_2(\text{dppe})(\text{H})_2$ (**2**) a series of NMR spectra were recorded at 193 K. The $^{31}\text{P}\{^1\text{H}\}$ NMR spectrum of **2** contains a pair of mutually coupled resonances at δ 92.4 and δ 97.8 ($J_{\text{P-P}} = 16$ Hz), due to two inequivalent phosphorus centres in the product. An assignment of the relative positions of the phosphorus ligands was made on the basis of nOe data and decoupling experiments as shown in Figure 2. It is interesting to note that the phosphorus atom that is *cis* to both hydride ligands yields the larger hydride phosphorus couplings. This differs from the situation at ruthenium where the *trans* hydride-phosphorus coupling is larger than a *cis* coupling, reinforcing the need for care to be taken when ligand arrangements are based on coupling data. A full description of the methods used in the characterisation can be found in the electronic supplementary

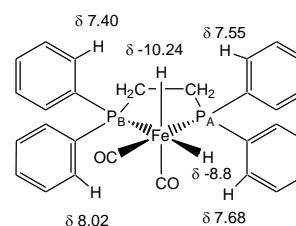


Figure 2. Representation of the structure for $\text{Fe}(\text{CO})_2(\text{dppe})(\text{H})_2$ **2** illustrating key NMR features.

information.[†]

Theoretical studies on the fragments $\text{Fe}(\text{CO})_2(\text{dpe})$ and $\text{Ru}(\text{CO})_2(\text{dpe})$. Recently, some of us have shown that 16-electron mixed phosphine and carbonyl $\text{Fe}(0)$ species of the type $\text{Fe}(\text{CO})_2(\text{PH}_3)_2$ do indeed have a triplet ground state³ like those of $\text{Fe}(\text{CO})_4$ and $\text{Fe}(\text{PR}_3)_4$.²¹ However, the use of chelating phosphines is known to change the reactivity of metal fragments dramatically because of the P-M-P bond angles that result. An appropriate theoretical study was therefore undertaken. The importance of this study was heightened by the fact that the electronic structure of the related complex, *cis-cis* $\text{Fe}(\text{CO})_2(\text{PH}_3)_2$, only optimised in the singlet even though the lowest energy *trans-cis* isomer $\text{Fe}(\text{CO})_2(\text{PH}_3)_2$ corresponded to a triplet.

Calculations were carried out on model complexes containing the $\text{PH}_2\text{CH}_2\text{CH}_2\text{PH}_2$ (dpe) ligand in place of dppe at the same level of theory previously employed for $\text{Fe}(\text{CO})_2(\text{PH}_3)_2$,²² since a benchmark investigation had shown this to give the most reliable results for $\text{Fe}(\text{CO})_4$.²² This corresponds to using B3PW91*, where the coefficient c_3 describing the mixing of the “exact”, Hartree-Fock, exchange is reduced to 0.15 (vs 0.20 in B3PW91). The 16-electron fragment $\text{Fe}(\text{CO})_2(\text{dpe})$ (**I**) was found to adopt a triplet ground state and possess a distorted trigonal bipyramid geometry with one vacant

equatorial site where the $P_{ax}-Fe-CO_{ax}$ angle was 156.0° and the $P_{eq}-Fe-CO_{eq}$ angle is 98.4° (Figure 3). Both the $Fe-P_{ax}$ distance of 2.271 \AA and the $Fe-CO_{ax}$ distance of 1.805 \AA in **I** proved to be longer than the corresponding equatorial distances of 2.240 \AA and 1.786 \AA respectively (Table 1). This trend is common in four coordinate systems with this geometry.

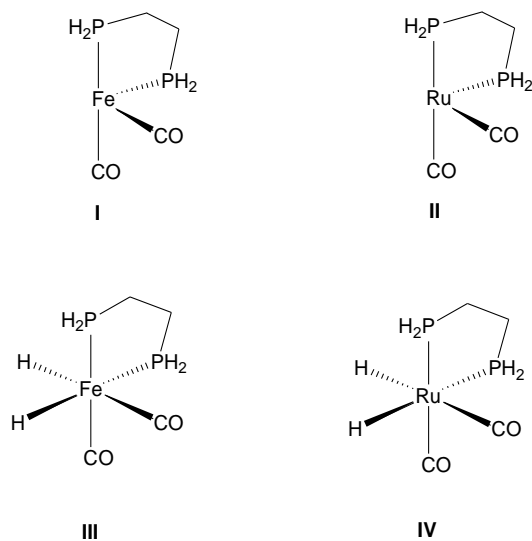


Figure 3. Labelling scheme for all calculated molecules.

Table 1. Calculated bond lengths (\AA) and angles (deg) for all species using the B3PW91* functional

Compound	M-L _{ax}	M-L _{eq}	H...H	L _{ax} - M-L _{ax}	L _{eq} - M-L _{eq}	H-M- H
H ₂	-	-	0.748	-	-	-
¹ Fe(CO) ₂ (dpe)	2.213(P) 1.755(C)	2.160(P) 1.733(C)	-	176.9	133.7	-
³ Fe(CO) ₂ (dpe)	2.271(P) 1.805(C)	2.240(P) 1.786(C)	-	156.0	98.4	-
^{1/3} Fe(CO) ₂ (dpe) + H ₂ (MECP)	2.307(P) 1.816(C)	2.272(P) 1.782(C)	0.775	157.1	97.4	22.2
Fe(CO) ₂ (dpe)(H) ₂	2.171(P) 1.751(C)	2.186(P) 1.769(C)	2.000	157.0	103.4	82.4
Fe(CO) ₂ (dpe)(H) ₂ TS1	2.198(P) 1.749(C)		0.868	84.6 (PFeP) 88.7 (CFeC) 150.2,152.0 (PFeC)		31.1
Fe(CO) ₂ (dpe)(H) ₂ TS2	2.192(P) 1.753(C)		0.859	84.2 (PFeP) 87.0 (CFeC) 151.0,151.6 (PFeC)		30.7
¹ Ru(CO) ₂ (dpe)	2.342(P) 1.878(C)	2.319(P) 1.868(C)	-	174.3	149.9	-
³ Ru(CO) ₂ (dpe)	2.359(P) 1.914(C)	2.298(P) 1.867(C)	-	159.6	97.6	-
Ru(CO) ₂ (dpe)(H) ₂	2.323(P) 1.887(C)	2.346(P) 1.919(C)	2.136	162.7	104.1	81.5
Ru(CO) ₂ (dpe)(H) ₂ TS1	2.342(P) 1.879(C)		0.863	82.3 (PRuP) 89.3 (CRuC) 150.0,151.7 (PRuC)		27.9
Ru(CO) ₂ (dpe)(H) ₂ TS2	2.330(P) 1.887(C)		0.853	82.1 (PRuP) 87.7 (CRuC) 150.9,151.7 (PRuC)		27.5

The singlet state of $Fe(CO)_2(dpe)$ (**1**) optimised with a similar distorted trigonal bipyramid geometry, and proved to lie 40 kJ mol^{-1} above the triplet ground state (Figure 4). Comparison of the singlet $P_{ax}-Fe-CO_{ax}$ and $P_{eq}-Fe-CO_{eq}$ angles (176.9° and 133.7° respectively) with those of the triplet (156.0° and 98.4° respectively) reveals that the structure distorts towards the trigonal bipyramid upon pairing the electrons. The corresponding ligand-metal bond lengths are shorter in the singlet (Table 1).

The corresponding bond angles for the singlet *cis-cis* isomer of $Fe(CO)_2(PH_3)_2$ where the phosphines are free to adopt a geometry that is not constrained by the chelate effect are 155.4° and 129.9° respectively.²¹ The major difference between the chelate and non-chelate structures therefore manifests itself in a change in the equatorial ligand orientation. The comparison of the bond lengths in the singlet and triplet forms reveals minimal differences.

The predicted energy difference between the singlet and triplet isomers of $Fe(CO)_2(dpe)$ (**1**) is of great significance to the photochemical driven *p*-H₂ addition studies, since the NMR experiments suggest that *p*-H₂ enhanced hydride resonances for $Fe(CO)_2(dppe)(H)_2$ should be observed if singlet $Fe(CO)_2(dppe)$ is formed. Hydride signals for the same species, $Fe(CO)_2(dppe)(H)_2$, formed from triplet- $Fe(CO)_2(dppe)$, overlap exactly with those derived from the singlet route since they would arise from chemically identical species but have normal signal strength. In the case of **1**, we have demonstrated that the enhancement factor approaches 10,000. Assuming that the

results are thermodynamically derived, the lack of enhancement observed in the chemistry of **2** implies that the equilibrium concentration of the singlet would have to be at most 10^{-5} that of the triplet, which in turn suggests an energy difference between spin states exceeding 15 kJ mol^{-1} . Taking account that the singlet is more reactive than the triplet, and assuming singlet and triplet states are able to interconvert faster than addition to the triplet, the minimum energy difference between states would have to be still larger to account for the absence of enhancement. This fits in with the theoretical values, which predict an energy difference between the spin isomers of almost 40 kJ mol^{-1} .

The $\text{Ru}(\text{CO})_2(\text{dpe})$ system **II** was previously investigated by Eisenstein *et al.* at a theory level quite similar to ours,²³⁻²⁴ but the investigation was limited to the singlet state. We find the triplet state to lie 58 kJ mol^{-1} higher in energy implying that it will not be populated at room temperature, mirroring the experimental study. Structurally, the same trends are observed for the singlet isomer which has wider bond angles and shorter bond lengths than the triplet species, as outlined in Table 1. In the computed structure of singlet (**II**), both Ru–P and Ru–C bond lengths are shorter for the equatorially bonded ligands, in agreement with greater back-bonding in those positions. The Ru–C distances are slightly shorter than those previously calculated for the same system²³ and in close agreement with those determined experimentally for the related unsaturated Ru(0) complex $\text{Ru}(\text{CO})_2(\text{P}^t\text{Bu}_2\text{Me})_2$ with *trans* phosphines (1.886(10) and 1.854(6) Å).²⁵⁻²⁶ Our calculation yields a wider $L_{\text{ax}}\text{--Ru--}L_{\text{ax}}$ and a narrower $L_{\text{eq}}\text{--Ru--}L_{\text{eq}}$ angle than those reported previously by Eisenstein *et al.*²⁴ The relatively important variations in these optimized parameters that result from minor changes in the theory level provide a sign of a relatively flat potential energy surface along this coordinate, as also suggested by a study of the related $\text{Ru}(\text{CO})_2(\text{PH}_3)_2$ system.²⁴ The singlet state of $\text{Ru}(\text{CO})_2(\text{dpe})$ has a similar $L_{\text{ax}}\text{--Ru--}L_{\text{ax}}$ angle to

$\text{Fe}(\text{CO})_2(\text{dpe})$ but a wider $L_{\text{eq}}\text{--Ru--}L_{\text{eq}}$ angle. The triplet states of $\text{Ru}(\text{CO})_2(\text{dpe})$ and $\text{Fe}(\text{CO})_2(\text{dpe})$ have similar angles. The angles in the singlet Ru complex are also rather different from those determined experimentally for complex $\text{Ru}(\text{CO})_2(\text{P}^t\text{Bu}_2\text{Me})_2$ (axial: $165.56(8)^\circ$; equatorial: $133.3(4)^\circ$), suggesting that the ground state geometry is highly affected by the phosphine (steric effect, constraint imposed by the backbone).

Theoretical treatment of $\text{Fe}(\text{CO})_2(\text{dpe})(\text{H})_2$ (III**) and $\text{Ru}(\text{CO})_2(\text{dpe})(\text{H})_2$ (**IV**).** The energy gains associated with the oxidative addition of H_2 to $\text{M}(\text{CO})_2(\text{dpe})$ [$\text{M} = \text{Ru}$ (**I**), Fe (**II**)] (Figure 4) show that, as expected, the reaction is more exothermic for Ru (124 kJ mol^{-1}) than Fe (97.9 kJ mol^{-1}). Since the two 16-electron fragments have different spin states, it is interesting to consider also the energy gain for the two species relating to the same spin state. The energy gain relative to the triplet intermediate is much smaller for Fe than for Ru, whereas the energy gain relative to the singlet intermediate is *greater* for Fe. The large decrease in the energy gain from the triplet state on going from Ru to Fe may be related to the much greater cost of pairing the electrons for the smaller Fe ion.

The $\text{Fe}(\text{CO})_2(\text{dpe})(\text{H})_2$ **III** product optimised with a distorted octahedral structure. In the calculated structure of **III**, the bond lengths for the axial phosphine and CO ligands are now shorter than the corresponding equatorial ligands (Table 1). This is consistent with the known *trans* influence of the hydride ligand. The basic structure is however similar to that reported for the related Fe(II) complex, *tcc*- $\text{Fe}(\text{CO})_2[\text{P}(\text{O}^i\text{Pr})_3]_2\text{H}_2$.²⁷⁻²⁸

In the calculated structure of (**III**), the $\text{P}_{\text{ax}}\text{--Fe--CO}_{\text{ax}}$ angle was found to be 157.0° , rather than the ideal value of 180° and the two groups are bent towards the hydrides ligands. In the equatorial plane the $\text{P}_{\text{eq}}\text{--Fe--CO}_{\text{eq}}$ angle widens to 103.4° with the H--Fe--H angle shrinking to 82.4° to accommodate this, although the $\text{H}\cdots\text{H}$ distance is 2.00 \AA . The distorted geometry is seen for $\text{Ru}(\text{CO})_2(\text{dpe})(\text{H})_2$ (**IV**), but in this case the bond

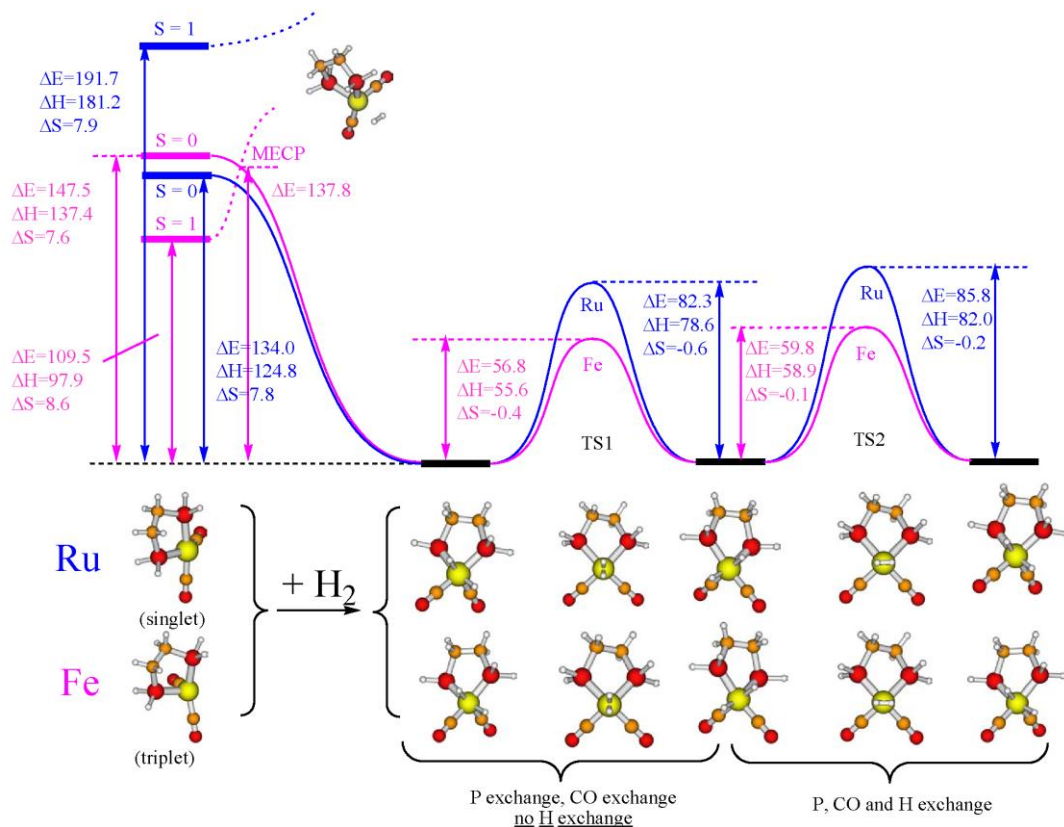


Figure 4. Calculated reaction coordinate, thermodynamic parameters and illustrations of the relevant geometries for the H_2 addition to $\text{M}(\text{CO})_2(\text{dpe})$ and for the ligand scrambling processes ($\text{M} = \text{Fe}$, Ru).

distances are longer than their iron counterparts (Table 1). This allows the $P_{ax}\text{-Ru-CO}_{ax}$ angle to increase to 162.7° so that the ruthenium structure distorts less from the ideal octahedral arrangement than the iron system. The $P_{eq}\text{-Ru-CO}_{eq}$ angle of 104° is essentially the same as that seen at iron although the H–Ru–H angle closes slightly to 81.5° . The greater Ru–H bond lengths result in a longer H...H contact of 2.136 \AA . It should be noted that no x-ray data are available for a monomeric Ru(II) complex of this type for comparison.

Minimum energy crossing point. The explicit determination of the MECP yields a structure whose geometry and energy are illustrated in Table 1 and Figure 4. This is closely related to the MECP for the H_2 addition to other 16-electron Fe(0) fragments.²¹ The H_2 ligand is found to approach the metal centre with a parallel orientation relative to the equatorial plane of the trigonal bipyramid and sideways relative to the empty coordination site. This preferred mode of attack was attributed to the greater repulsion by the a_1 orbital relative to the b_1 orbital of the ideal C_{2v} FeL_4 fragment.

For the previously reported $^{1/3}FeL_4+H_2$ MECPs, it was found that the $Fe\cdots H$ distance decreases and the $H\cdots H$ distance increases with an increase of the ligand's donor strength.²¹ However, the calculated $Fe\cdots H$ distances of 1.997 \AA and 2.031 \AA and the $H\cdots H$ distance of 0.775 \AA for the crossing point of the $Fe(CO)_2(dpe)$ system are quite close to those of the electronically similar $Fe(CO)_2(PH_3)_2$ system, for which the comparative $Fe\cdots H$ distances are 1.981 and 2.052 \AA , and the $H\cdots H$ distance is 0.778 \AA .²¹ Energetically, the MECP is located 28.3 kJ mol^{-1} higher than the triplet $Fe(CO)_2(dpe)$ fragment, a value similar to those of the FeL_4 systems investigated previously. In a recent contribution, we computed a singlet/triplet energy splitting of 50.2 kJ mol^{-1} for $Fe(dmpe)_2$ and of 62.1 kJ mol^{-1} for $Fe(dpe)_2$.²¹ In the latter case, the MECP lies 25.6 kJ mol^{-1} above the reactants which is similar to the 28.3 kJ mol^{-1} found here. Similar rate coefficients for H_2 addition would therefore be expected for the two systems. The $Fe(dmpe)_2$ system was found to react with H_2 with a rate constant of $8 \times 10^5 \text{ dm}^3 \text{ mol}^{-1} \text{ s}^{-1}$ at room temperature.²⁹ Based on the failure to detect any enhanced hydride resonance we would predict the lifetime of the triplet at 195 K to be less than 1 ms .

Fluxionality with $Ru(CO)_2(dppe)(H)_2$ and $Fe(CO)_2(dppe)(H)_2$. While the 1H NMR spectrum of *ccc*- $Fe(CO)_2(dppe)(H)_2$ **2** contained two inequivalent hydride signals at 245 K upon warming to 295 K a single broad peak is observed at $\delta -9.9$. The corresponding $^{31}P\{^1H\}$ spectrum also consists of a very broad signal centred at $\delta 96$ at this temperature showing that $Fe(CO)_2(dppe)(H)_2$ is highly fluxional. Line shape analysis was used to determine the rate of exchange of the hydride ligands in *ccc*- $Fe(CO)_2(dppe)(H)_2$. For this purpose, 1H NMR spectra were recorded at intervals of around 5 K between 189 K to 296 K in toluene- d_8 solution. Spectra were then analysed using g-NMR³⁰ and rates obtained for data between 216 K and 270 K . In order to improve the number of reliable temperatures, a coalescence measurement was also employed which allowed the hydride ligand exchange rate at 271.3 K to be determined as 1300 s^{-1} . Rate data are provided in the ESI.[†] The activation parameters for the hydride ligand exchange process were determined to be $\Delta H^\ddagger = 48 \pm 6 \text{ kJ mol}^{-1}$ and $\Delta S^\ddagger = -10 \pm 20 \text{ J mol}^{-1} \text{ K}^{-1}$ for this process.

Line shape analysis of the corresponding $^{31}P\{^1H\}$ spectra between 200 K and 290 K was used to examine the phosphorus interchange pathway. The activation parameters for this process were calculated to be $\Delta H^\ddagger = 33 \pm 5 \text{ kJ mol}^{-1}$ and $\Delta S^\ddagger = -48 \pm 20 \text{ J mol}^{-1} \text{ K}^{-1}$ and are substantially different from those for hydride interchange. The observation that the phosphorus interchange process has the lower activation barrier is consistent with rates of 90 s^{-1} and 24 s^{-1} respectively that were determined for the two pathways at 232 K . This suggests that phosphorus and hydride interchange can occur independently of one another.

Theory indicated that there are two possible ways of exchanging the hydride ligands in $M(CO)_2(dpe)(H)_2$ [$M = Ru, Fe$] (Figure 4). The two pathways can be described as pseudo-rotations involving the two hydride ligands, each one occurring in a different direction (clockwise and anticlockwise). One route (through the transition state **TS1**) involves only P and CO site interchange, with the hydride ligands remaining unaffected. In the second pathway (through **TS2**), all three sets of ligands exchange sites simultaneously. In the iron system, the calculated enthalpy change to reach **TS1** (ΔH^\ddagger) from the ground state was found to be $+55.6 \text{ kJ mol}^{-1}$, while for **TS2** the enthalpy is higher at $+58.9 \text{ kJ mol}^{-1}$. This is consistent with the experimental observation that P-P mutual exchange has the lower activation barrier. However, the experimental activation enthalpies are substantially lower than those calculated for both processes which suggests that a steric effect arising from the phenyl substituents is not fully represented in the calculations where they are replaced by hydrogen at the small iron centre.

The calculated entropy change (ΔS^\ddagger) for these processes were found to be slightly negative as shown in Figure 4 and indicates that there is little or no change in order on moving from the ground state to the transition state. Negative entropy terms were also obtained by experiment, although the errors are substantial. The related complex $Fe(CO)_2\{(C_2F_5)_2P(CH_2CH_2P(C_2F_5)_2)(H)_2\}$ has been prepared by Brookhart *et al.* in a similar manner.³¹ This complex also proved to be stereochemically nonrigid with the hydride exchange rate being estimated at $3.2 \times 10^3 \text{ s}^{-1}$ at 235 K . Slower, phosphorus site exchange was also observed ($4 \times 10^3 \text{ s}^{-1}$ at 257 K).

Some of us have previously shown that *ccc*- $Ru(CO)_2(dppe)(H)_2$ is fluxional, undergoing intramolecular exchange of the two hydride ligands on the NMR timescale.¹⁸ Quantitative analysis of this behaviour led us to suggest that hydride interchange was accompanied by synchronised exchange of the two carbonyl ligands and the dppe phosphorus atoms. We proposed that this process involves accessing a five coordinate complex containing an $\eta^2\text{-H}_2$ ligand which, in view of the small normal kinetic isotope effect and apparently restricted rotation had only a weak H-H interaction. This deduction was based on the observation that at 306.2 K , the rates of hydride, phosphorus and carbonyl interchange were the same within experimental error suggesting synchronised exchange. The activation parameters were as follows: $\Delta H^\ddagger = 85.5 \pm 2 \text{ kJ mol}^{-1}$ and $\Delta S^\ddagger = 34 \pm 7 \text{ J mol}^{-1} \text{ K}^{-1}$ and a ΔG^\ddagger value of 75 kJ mol^{-1} .¹⁸

We have now carried out calculations on **IV** that predict two independent ligand exchange pathways exist for **1** in direct analogy with **2**. The corresponding calculated enthalpies of activation for **TS1** and **TS2** are 78.6 kJ mol^{-1} and 82.0 kJ mol^{-1} , very close to the experimental values for hydride ligand exchange in **IV**. The experimentally determined ΔS^\ddagger value of $34 \pm 7 \text{ J mol}^{-1} \text{ K}^{-1}$ is, however, significantly different from the zero value predicted theoretically. Clearly, the entropy effects are not adequately modelled using this level of theory. The H–H bond distances in **TS1** and **TS2** for **III** and **IV** are in the range seen for $\eta^2\text{-H}_2$ ligands, those of **TS1** (0.868 and 0.863 \AA for Fe and Ru, respectively) being only slightly longer than those of **TS2** (0.859 and 0.853 \AA). These distances suggest that both exchange processes place the hydride ligands sufficiently close together for the formation of a five coordinate geometry with a metal-bonded “dihydrogen” ligand. However, no local minimum corresponding to such complex was found; thus no distinct dihydrogen intermediates exist along the exchange pathways.

Reductive elimination of H_2 from $Ru(CO)_2(dppe)(H)_2$ and $Fe(CO)_2(dppe)(H)_2$. We have previously described¹⁸ how exchange between metal dihydride and free dihydrogen involving **1** can be examined quantitatively over the temperature range $343\text{--}373 \text{ K}$ via the mapping of hydride/dihydrogen connections obtained as a function of mixing time using the ID-nOe sequence of Keeler.³² Subsequent analysis provided values of $\Delta H^\ddagger = 97 \pm 10 \text{ kJ mol}^{-1}$ and $\Delta S^\ddagger = 2 \pm 2 \text{ J mol}^{-1} \text{ K}^{-1}$ for this

reaction. At 369 K the rate of reductive elimination of H₂ from **1** was 0.253 s⁻¹. As can be seen from Figure 4, this experimental enthalpy is higher than that calculated for **TS1/TS2**, but much lower than that calculated to reach singlet Ru(CO)₂(dpe). This suggests that the reductive elimination step is not purely dissociative.

When the reaction of Fe(CO)₂(dppe)(H)₂ was monitored in a similar way, no exchange peaks to free H₂ were observed up to 363 K, the highest readily accessible temperature. The failure to detect magnetisation transfer to H₂ could be attributed either to paramagnetic quenching of the associated spin encoding, or to a process which was too slow to observe on the timescale of the EXSY experiment. We therefore examined the reaction of **2** with CO to form the precursor Fe(CO)₃(dppe) by NMR spectroscopy at 333 K. A slow exponential decay of the signal due to the hydride resonances of **2** was observed which yielded a first order rate constant of 6 × 10⁻⁵ s⁻¹, or ΔG[‡] = 109 kJ mol⁻¹ at 333 K. This observation requires slow H₂ elimination from **2**. In the case of Fe(CO)₂{(C₂F₅)₂PCH₂CH₂P(C₂F₅)₂}(H)₂, Brookhart *et al.* reported that trapping of the H₂ loss product with P(OMe)₃, proceeded at the substantially faster rate of 7 × 10⁻³ s⁻¹ at 252 K. This confirms that the use of the fluorinated phosphine destabilises the Fe(II) centre and aids in H₂ elimination.³¹

Conclusions

Literature studies on the laser-initiated reaction of Ru(CO)₃(dmpe) (dmpe = Me₂PCH₂CH₂PMe₂) with H₂ have described how CO dissociation leads to the rapid formation of Ru(CO)₂(dmpe)(solvent). On a longer timescale, reaction with H₂ leads to the generation of the stable complex Ru(CO)₂(dmpe)(H)₂.³³ We have described how this route can be used to prepare the analogous complex, Ru(CO)₂(dppe)(H)₂ (**1**) from the readily accessible precursor Ru(CO)₃(dppe) and then extended this approach to Fe(CO)₃(dppe) and hence prepared Fe(CO)₂(dppe)(H)₂.

The proposed role of the zerovalent d⁸ intermediates, Ru(CO)₂(dppe) and Fe(CO)₂(dppe), in these reactions is in keeping with related Ru(CO)₅ and Ru(PR₃)₄(H)₂ systems which feature Ru(CO)₄ and Ru(PR₃)₄ intermediates.¹⁻⁴ The reactivity of such species is, however, influenced dramatically by the electron configuration, be it singlet or triplet, which in turn depends on the strength of interaction between the metal and ligand. In the case of the related complexes Fe(CO)₄, Fe(PH₃)₄ and more recently Fe(CO)₂(PH₃)₂, it has been established by appropriate theory that triplet ground states are adopted.²¹ The energy difference between the triplet and the singlet reduces as the σ-donor properties of the phosphine increase, and the π-accepting properties of the ligands increase. The resultant need for spin crossover during reactions producing diamagnetic 18 electron products necessitates an increased activation barrier and hence a slower reaction rate. The analogous Ru(CO)₄ and Ru(PH₃)₄ complexes on the other hand have been shown to adopt singlet ground states.

Here we have studied the reactions of the intermediates Ru(CO)₂(dppe) and Fe(CO)₂(dppe) with *p*-H₂ by NMR spectroscopy. Evidence has been presented that when Fe(CO)₂(dppe) reacts to form Fe(CO)₂(dppe)(H)₂, no signal enhancements are observed for the corresponding hydride ligand signals. In contrast when Ru(CO)₂(dppe) is used, signal enhancements are observed for the analogous hydride resonances of Ru(CO)₂(dppe)(H)₂. This result is consistent with the fast reaction of a diamagnetic complex leading to retention of the nuclear spin encoding and generation of **1** which retains *p*-H₂ activity. When Fe(CO)₃(dppe) is irradiated however, the triplet or paramagnet, Fe(CO)₂(dppe), adds H₂ with concomitant loss of the spin-encoding due to enhanced relaxation.³⁴ This simple observation demonstrates that the electronic spin state of a reaction centre can be probed readily in conjunction with a suitable nuclear spin reservoir such as *p*-H₂. Furthermore, it

suggests that when substantial *p*-H₂ enhancements have been observed the reaction pathways involve diamagnetic centres. Since the studies in CD₃CN produced similar results, we suggest that these reactions proceed via direct H₂ addition to the naked 16-electron fragment, rather than associative displacement from the 18 electron solvent complex.

Given the propensity for chelate structures to influence reactivity, we completed a B3PW91* study of the structures of Ru(CO)₂(dpe) and Fe(CO)₂(dpe) (where dpe = PH₂CH₂CH₂PH₂). As expected, the iron system proved to be a triplet while the ruthenium complex was a singlet. The energy difference between the iron triplet, and the excited singlet was determined to be 40 kJ mol⁻¹. This value is sufficiently large to account for the failure to see enhancement from a small equilibrium amount of the singlet.

The NMR data for both **1** and **2** indicated that they are fluxional on the NMR timescale. In the case of **1**, a series of ¹H, ³¹P and ¹³C, studies revealed an apparently synchronised interchange of the hydride, phosphine and carbonyl pairs. Measured activation parameters for these processes were ΔH[‡] = 85.5 ± 2 kJ mol⁻¹ and ΔS[‡] = 34 ± 7 J mol⁻¹ K⁻¹. When this process was modelled for the dpe analogue, two pathways were revealed, one where the phosphorus and carbonyl centres alone interchange positions, and one where all three groups interchange. The theoretical activation enthalpies for these processes were ΔH[‡] = 78.6 kJ mol⁻¹ and ΔH[‡] = 82 kJ mol⁻¹ respectively. Our NMR observations failed to distinguish these two pathways and suggest that the calculations on the model complex underestimate the barrier to reaction in the case of **1** by about 7 kJ mol⁻¹ and that the two processes have similar activation barriers. The role of an η²-H₂ interaction in many hydride exchange processes has been suggested with H–H bond lengths between 0.8 and 1.0 Å in the transition states. Our calculations reveal that the H...H distance changes from 2.136 Å in **1** to 0.853 Å in the transition state for the hydride interchange pathway. This is consistent with increased H–H bonding character, although no local minimum (intermediate) was found along the rearrangement pathway.

In the case of **2**, the measured ΔH[‡] barrier to hydride interchange proved to be 48 ± 6 kJ mol⁻¹ while a second pathway that exchanges P and CO but not H has a ΔH[‡] barrier of 33 kJ mol⁻¹. The calculated values of 55.6 kJ mol⁻¹ and 58.9 kJ mol⁻¹ for the two analogous processes in Fe(CO)₂(dpe)(H)₂ seem to overestimate the barriers. The calculations, however, agree with the observation that the iron system is more fluxional. For the iron system **II**, the H...H distance changes from 2.00 Å to 0.859 Å in the transition state, which again suggests an increase in H–H bonding character.

Studies on the reductive elimination of H₂ from **1** yielded activation parameters of ΔH[‡] = 97 ± 10 kJ mol⁻¹ and ΔS[‡] = 2 ± 2 J K⁻¹ mol⁻¹ for this reaction. In contrast, the calculations indicated a barrier to H₂ loss of 124.8 kJ mol⁻¹. The low experimental barrier can be explained by a role for the solvent or the incoming ligand in stabilising the transition state. In other words, H₂ substitution is not purely dissociative in character.

Acknowledgements

We are grateful to the European Union for partial funding under the HYDROCHEM network (contract HPRN-CT-2002-00176) and to CINES for a grant of free computational time. Support from the University of York, the ERASMUS programme and the EPSRC is also acknowledged.

Experimental

Computational details. All calculations were performed using the Gaussian 98 program³⁵ together with the modified form of the B3PW91 functional in which the proportion of exact exchange has been modified from 0.20 to 0.15.²² We also used

flexible polarised basis sets on all atoms, as in our previous work on related systems.²¹⁻²² Thus, for Fe, C and O and P, and the incoming H₂ ligand, the triple-zeta basis sets of Schäfer *et al* were used,³⁶ with additional polarization functions. For other hydrogen atoms, the smaller split-valence basis of the same authors was used. Finally, for ruthenium, the 28 core electrons were treated using the ECP³⁷ with the valence electrons treated using the associated SDD basis set, augmented by one f polarisation function ($\alpha = 1.$) All minima and transition states were fully optimised and characterised by computing vibrational frequencies at the same level of theory. The MECF was located using Gaussian 98, together with the code developed by one of the authors.³⁸

Experimental details: The syntheses of Ru(CO)₃(dppe)³⁹ and Fe(CO)₃(dppe)⁴⁰ were performed according to literature methods. The complex Ru(CO)₂(dppe)(H)₂ (**1**) was obtained by *in-situ* irradiation of a toluene-d₈ solution of Ru(CO)₃(dppe) using a Kimmon 40 mW He/Cd CW laser in the presence of 3 atmospheres of *p*-H₂.¹⁶ The preparation of the Fe(CO)₂(dppe)(H)₂ used here was achieved by first converting Fe(CO)₅ by reaction with HSiPh₃ to Fe(CO)₄(SiPh₃)H.⁴¹ This white compound was then dissolved in benzene and 1 equivalent of dppe added. Argon was bubbled through the solution over 2 hrs to drive off the CO that is released. Upon concentration, the solution yielded an orange solid which was recrystallised from warm Et₂O, to yield yellow crystals of Fe(CO)₂(dppe)(H)₂. This procedure has been reported previously.⁴²

The toluene-d₈ (Apollo Scientific) was dried over potassium and degassed prior to use. The NMR measurements were made using NMR tubes fitted with J. Young Teflon valves and solvents were added by vacuum transfer on a high vacuum line. For the parahydrogen induced polarization (PHIP) experiments, hydrogen enriched in the *para* spin state was prepared by cooling H₂ to 77 K over a paramagnetic catalyst (Fe₂O₃) as previously described.¹⁴ Spectra were recorded on a Bruker DSX 400 spectrometer with ¹H at 400.13 MHz and ³¹P at 161.9 MHz. ¹H NMR chemical shifts are reported in ppm relative to residual ¹H signals in the deuterated solvents (toluene-d₇, δ 2.13, ³¹P NMR chemical shifts are relative to an external 85% solution of phosphoric acid.

References

† Electronic supplementary information (ESI) available: Cartesian coordinates for all optimised geometries, NMR parameters for Fe(CO)₂(dppe)(H)₂ and rate data for ligand interchange. See <http://www.rsc.org/suppdata/dt/>

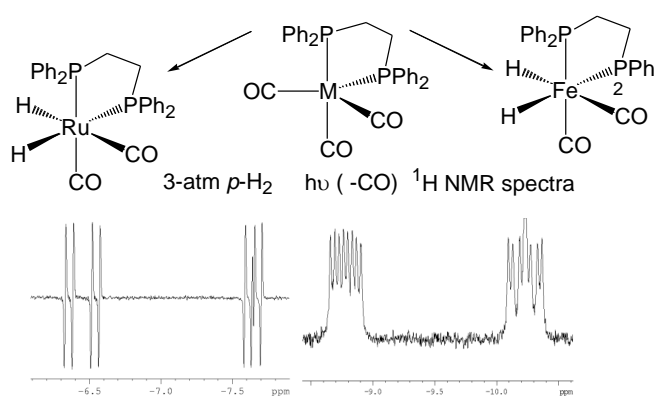
- 1 M. Poliakoff and E. Weitz, *Acc. Chem. Res.*, 1987, **20**, 408.
- 2 W. Wang, A. A. Narducci, P. G. House and E. Weitz, *J. Am. Chem. Soc.*, 1996, **118**, 8654.
- 3 P. T. Snee, C. K. Payne, S. D. Mebane, K. T. Kotz, and C. B. Harris, *J. Am. Chem. Soc.*, 2001, **123**, 6909.
- 4 H. Ihee, J. M. Cao and A. H. Zewail, *Angew. Chem., Int. Ed.*, 2001, **40**, 1532.
- 5 R. J. Rytter and E. Weitz, *J. Phys. Chem.*, 1991, **95**, 9841.
- 6 (a) J. Chetwynd-Talbot, P. Grebenik and R. N. Perutz, *Inorg. Chem.*, 1982, **21**, 3647. (b) P. A. Cox, P. Grebenik, R. N. Perutz, M. D. Robinson, R. Grinter and D. R. Stern, *Inorg. Chem.*, 1983, **22**, 3614. (c) R. G. Graham, R. Grinter and R. N. Perutz, *J. Am. Chem. Soc.*, 1998, **110**, 7036. (d) F. G. N. Cloke, J. C. Green., M. L. H. Green and C. P. Morley, *Chem. Commun.*, 1985, 945. (e) see L. Labella, A. Chernega and M. L. H. Green, *J. Chem. Soc. Dalton Trans.*, 1995, 395 and reference therein.
- 7 (a) J. C. Green, J. N. Harvey and R. Poli, *Dalton Trans.*, 2002, 1861. (b) J. C. Green, *Chem. Soc. Rev.*, 1998, **27**, 263.
- 8 (a) A. A. Bengali, R. G. Bergman and C. B. Moore, *J. Am. Chem. Soc.*, 1995, **117**, 3879. (b) P. T. Snee, C. K. Payne, C. T. Kotz, H. Yang and C. B. Harris, *J. Am. Chem. Soc.*, 2001, **123**, 2255.
- 9 R. Poli and K. M. Smith, *Eur. J. Inorg. Chem.*, 1999, **12**, 877.
- 10 C. Hall and R. N. Perutz, *Chem Rev.*, 1996, **96**, 3125.

- 11 C. R. Bowers, D. H. Jones, N. D. Kurur and J. A. Labinger, *Adv. Magn. Reson.*, 1990, **14**, 269.
- 12 R. Eisenberg, *Acc. Chem. Res.*, 1991, **24**, 100.
- 13 J. Natherer and J. Bargon, *Prog. Nucl. Magn. Res.*, 1997, **31**, 293.
- 14 S. B. Duckett and C. J. Sleigh, *Prog. Nucl. Magn. Res.*, 1999, **34**, 71
- 15 S. B. Duckett and D. Blazina, *Eur. J. Inorg. Chem.*, 2003, **16**, 2901.
- 16 C. Godard, P. Callaghan, J. L. Cunningham, S. B. Duckett, J. A. B. Lohman and R. N. Perutz, *Chem. Commun.* 2002, 2836.
- 17 (a) S. Geftakis and G. E. Ball, *J. Am. Chem. Soc.*, **1999**, **121**, 6336. (b) N. A. Knatochnil, J. A. Pachinson, P. J. Bedmaishi and P. J. Sadler, *Angew. Chem. Int. Ed.* 1999, **38**, 1460. (c) C. E. Lyon, J. L. Lopez, B-M. Cho and P. J. Hore, *Mol. Phys.* 2002, **100**, 1261. (d) T. Kühn and H. Schwalbe, *J. Am. Chem. Soc.* 2002, **122**, 6169.
- 18 D. Schott, C. J. Sleigh, J. P. Lowe, S. B. Duckett, R. J. Mawby and M. G. Partridge, *Inorg. Chem.*, 2002, **41**, 2960.
- 19 (a) G. E. Ball and B. E. Mann, *J. Am. Chem. Soc., Chem. Commun.*, 1992, 561 (b) P. Meakin, E. L. Muetterties and J. P. Jesson, *J. Am. Chem. Soc.*, 1973, **95**, 75.
- 20 U. Schubert and M. Knorr, *Inorg. Chem.*, 1989, **28**, 1765.
- 21 J. N. Harvey and R. Poli, *Dalton Trans.*, 2003, **21**, 4100.
- 22 J. Harvey and M. Aschi, *Faraday Disc.*, 2003, **124**, 129.
- 23 T. Gottschalk-Gaudig, J. C. Huffman, K. G. Caulton, H. Gerard and O. Eisenstein, *J. Am. Chem. Soc.*, 1999, **121**, 3242.
- 24 T. Gottschalk-Gaudig, J. C. Huffman, H. Gérard, O. Eisenstein and K. G. Caulton, *Inorg. Chem.*, 2000, **39**, 3957.
- 25 M. Ogasawara, S. A. MacGregor, W. E. Streib, K. Folting, O. Eisenstein and K. G. Caulton, *J. Am. Chem. Soc.*, 1995, **117**, 8869.
- 26 M. Ogasawara, S. A. MacGregor, W. E. Streib, K. Folting, O. Eisenstein and K. G. Caulton, *J. Am. Chem. Soc.*, 1996, **118**, 10189.
- 27 V. Arion, J. J. Brunet and D. Neibecker, *Inorg. Chem.*, 2001, **40**, 2628.
- 28 Nan Nhat Ho, R. Bau and S. A. Mason, *J. Organomet. Chem.*, 2003, **676**, 85.
- 29 M. K. Whittlesey, R. J. Mawby, R. Osman, R. N. Perutz, L. D. Field, M. P. Wilkinson and M. W. George, *J. Am. Chem. Soc.*, 1993, **115**, 8627.
- 30 G-NMR V5. Adept Scientific. Plc 2003.
- 31 M. Brookhart, W. A. Chandler, A. C. Pfister, C. C. Santini and P. S. White, *Organometallics*, 1992, **11**, 1263.
- 32 K. Stott, J. Stonehouse, J. Keeler, T. L. Hwang and A. J. Shaka, *J. Am. Chem. Soc.*, 1995, **117**, 4199.
- 33 M. K. Whittlesey, R. N. Perutz, I. P. Virrels and M. W. George, *Organometallics*, 1997, **16**, 268.
- 34 T. Nilsson and J. Kowalewski *Mol. Phys.* 1617, **98**, 2000.
- 35 Gaussian 98, Revision A.11.1, M. J. Frisch, G. W. Trucks, H. B. Schlegel, G. E. Scuseria, M. A. Robb, J. R. Cheeseman, V. G. Zakrzewski, J. A. Montgomery, Jr., R. E. Stratmann, J. C. Burant, S. Dapprich, J. M. Millam, A. D. Daniels, K. N. Kudin, M. C. Strain, O. Farkas, J. Tomasi, V. Barone, M. Cossi, R. Cammi, B. Mennucci, C. Pomelli, C. Adamo, S. Clifford, J. Ochterski, G. A. Peterson, P. Y. Ayala, Q. Cui, K. Morokuma, P. Salvador, J. J. Dannenberg, D. K. Malick, A. D. Rabuck, K. Raghavachari, J. B. Foresman, J. Cioslowski, J. V. Ortiz, A. G. Baboul, B. B. Stefanov, G. Liu, a. Liaskenko, P. Piskorz, I. Komaromi, R. Gomperts, R. L. Martin, D. J. Fox, T. Keith, M. A. Al-Laham, C. Y. Peng, A. Nanayakkara, M. Challacombe, P. M. W. Gill, B. Johnson, W. Chen, M. W. Wong, J. L. Andres, C. Gonzalez. M. Head-Gordon, E. S. Replogle and J. A. Pople, Gaussian, Inc., Pittsburgh PA, 2001.
- 36 A. Schaefer, H. Horn and R. Ahlrichs, *J. Chem. Phys.*, 1992, **97**, 2571.
- 37 D. Andrae, U. Haussermann, M. Dolg, H. Stoll and H. Preuss, *Theor. Chim. Acta*, 1990, **77**, 123.
- 38 J. N. Harvey, M. Aschi, H. Schwarz and W. Koch, *Theor. Chem. Acc.*, 1998, **99**, 95.
- 39 R. A. Sanchez-Delgado, J. S. Bradley, G. Wilkinson, *J. Chem. Soc. Dalton Trans.*, 1976, **5**, 399.
- 40 T. A. Manuel *Inorg. Chem.*, 1963, **2**, 854.
- 41 W. Jetz and W. A. G. Graham, *Inorg. Chem.*, 1971, **10**, 4.
- 42 U. Shuburt and M. Knorr, *Inorg. Chem.*, 1989, **29**, 1675..

Graphical Abstract

The reaction of $M(\text{CO})_3(\text{Ph}_2\text{PCH}_2\text{CH}_2\text{PPh}_2)$ ($M = \text{Fe}, \text{Ru}$) with parahydrogen: probing the electronic structure of reaction intermediates and the internal rearrangement mechanism for the dihydride products

Danièle Schott,^a Philip Callaghan,^a John Dunne,^a Simon B. Duckett,^{a*} Cyril Godard,^a José M. Goicoechea,^d Jeremy N. Harvey,^b Roger J. Mawby,^a Georg Müller,^a Robin N. Perutz,^a Rinaldo Poli^c and Michael K. Whittlesey^d



On *in-situ* photoysis of $M(\text{CO})_3(\text{dppe})$ with parahydrogen normal ^1H NMR hydride signals are recorded for $\text{Fe}(\text{CO})_2(\text{dppe})(\text{H})_2$ and enhanced hydride signals for $\text{Ru}(\text{CO})_2(\text{dppe})(\text{H})_2$. This effect is associated with a singlet electronic state of $\text{Ru}(\text{CO})_2(\text{dppe})$ while $\text{Fe}(\text{CO})_2(\text{dppe})$ is a triplet. Calculations reveal electronic ground states consistent with this picture.